AD-A038 557 EG AND G INC SALEM MASS ELECTRONIC COMPONENTS DIV F/G 9/1
REPETITIVE SERIES INTERRUPTER II.(U)
MAR 77 R SIMON, D V TURNQUIST DAAB07-76-C-1301
UNCLASSIFIED ECOM-76-1301-2 NL

1 OF 1
ADA038557

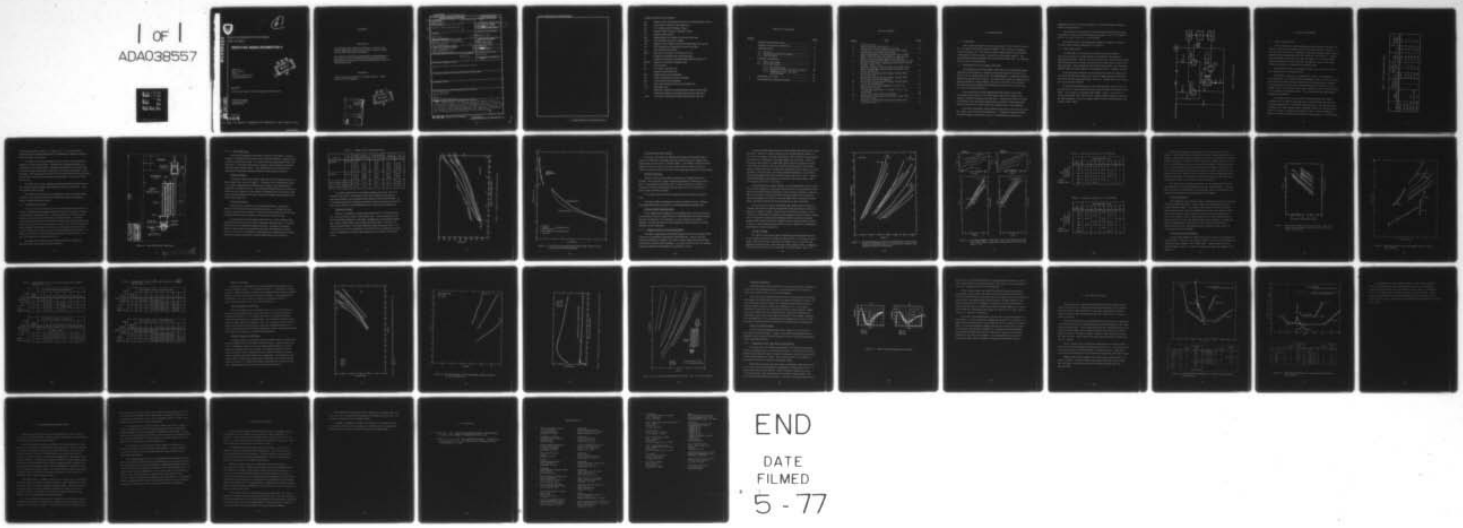

END

DATE FILMED
5 - 77

Research and Development Technical Report

ECOM -76-1301-2

REPETITIVE SERIES INTERRUPTER II

Robert Simon
David V. Turnquist
EG&G Inc.
Electronic Components Division
Salem, Massachusetts 01970

March 1977

Second Triannual Report for the Period 23 May 1976 to 31 December 1976

Prepared for:

ECOM

US ARMY ELECTRONICS COMMAND FORT MONMOUTH, NEW JERSEY 07703

NOTICES

Disclaimers

The findings in this report are not to be construed as an official Department of the Army position, unless so designated by other authorized documents.

The citation of trade names and names of manufacturers in this report is not to be construed as official Government indorsement or approval of commercial products or services referenced herein.

Disposition

Destroy this report when it is no longer needed. Do not return it to the originator.

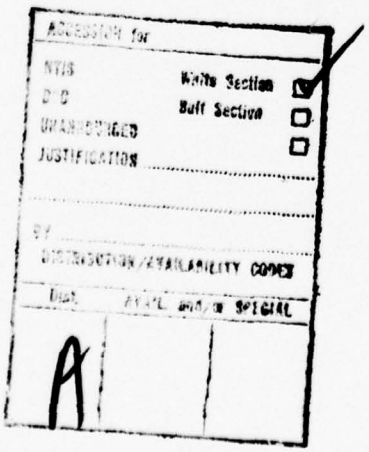

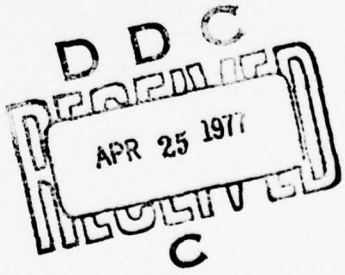

UNCLASSIFIED

SECURITY CLASSIFICATION OF THIS PAGE (When Data Entered)

REPORT DOCUMENTATION PAGE

READ INSTRUCTIONS BEFORE COMPLETING FORM

1. REPORT NUMBER: ECOM-76-1301-2	2. GOVT ACCESSION NO.
3. RECIPIENT'S CATALOG NUMBER	
4. TITLE (and Subtitle): Repetitive Series Interrupter II.	5. TYPE OF REPORT & PERIOD COVERED: Second Triannual Report, no. 2, 23 May [illegible]-31 Dec 76
	6. PERFORMING ORG. REPORT NUMBER
7. AUTHOR(s): Robert Simon, David V. Turnquist	8. CONTRACT OR GRANT NUMBER(s): DAAB07-76-C-1301
9. PERFORMING ORGANIZATION NAME AND ADDRESS: EG&G Inc., Electronic Components Div., 35 Congress Street, Salem, Massachusetts 01970	10. PROGRAM ELEMENT, PROJECT, TASK AREA & WORK UNIT NUMBERS: 62705, 1L762705AH94AE1.01
11. CONTROLLING OFFICE NAME AND ADDRESS: US Army Electronics Command, ATTN: DRSEL-TL-BG, Fort Monmouth, NJ 07703	12. REPORT DATE: Mar[illegible]977
	13. NUMBER OF PAGES: 45
14. MONITORING AGENCY NAME & ADDRESS (if different from Controlling Office): 44p.	15. SECURITY CLASS. (of this report): Unclassified
	15a. DECLASSIFICATION/DOWNGRADING SCHEDULE

16. DISTRIBUTION STATEMENT (of this Report)

Approved for Public Release; Distribution Unlimited

17. DISTRIBUTION STATEMENT (of the abstract entered in Block 20, if different from Report)

18. SUPPLEMENTARY NOTES

19. KEY WORDS (Continue on reverse side if necessary and identify by block number)

Series Interrupter
Gas Filled Device
Fuse
Thyratron
Magnetic Interaction Region

20. ABSTRACT (Continue on reverse side if necessary and identify by block number)

This report describes work done from May through December, 1976 on the Repetitive Series Interrupter, a hydrogen thyratron modified for switch-opening operation. Parametric studies of tube behavior, particularly of tube voltage drop and current-quenching requirements, are given, with further notes of tube performance and operational characteristics. Experimental modifications are mentioned and proposed continuations of work are discussed.

DD FORM 1 JAN 73 1473 EDITION OF 1 NOV 65 IS OBSOLETE

UNCLASSIFIED

SECURITY CLASSIFICATION OF THIS PAGE (When Data Entered)

410 029

ABBREVIATIONS AND SYMBOLS

Bq	Magnetic field (kilogauss) required for quenching fault current
Ebb	Main supply voltage for tube under test
Ef	TUT cathode heater filament voltage
$\mathscr{E}_j$	Magnetic field energy for RSI tube volume
Em	Magnet supply voltage
epy	Instantaneous full voltage across tube under test
Eres	TUT hydrogen reservoir voltage
Eq	Magnet circuit voltage required for quenching fault current
etd	TUT voltage drop during normal pulse operation
ib	Peak RSI-carried current
iRSI	RSI-carried current, as a function of time
L	Length of interaction tube used during test
m	Empirical exponent of proportionality between Bq and 1/L
MCCD	Magnetic-Controlled Charging Diode
P	TUT pressure
prr	TUT pulse repetition rate
r	Radius of interaction tube
Rm	Magnet circuit load resistance
Rl	Pulse-forming network load resistance
Rrc	Fault network load resistance
τD	Time delay between TUT fire and magnet fire
TUT	Tube under test
β	Empirical exponent of proportionality between Bq and Ebb
δ	Empirical exponent of proportionality between Bq and ib
Δ tad	Full range of deviation of delay time drift for tube fire

TABLE OF CONTENTS

LIST OF FIGURES

1. INTRODUCTION

1.1 FOREWORD

This report documents work performed from 23 May 1976 to 31 December 1976 under USAECOM Contract DAAB07-C-1301, entitled " Repetitive Series Interrupter II." This is the Second Triannual Report, representing a continuation of work previously reported (First Triannual Report). The investigations herein described were performed by EG&G, Inc., 35 Congress Street, Salem, Massachusetts.

1.2 BACKGROUND AND GENERAL RESULTS

The Repetitive Series Interrupter (RSI) tubes are hydrogen thyratrons adapted by the inclusion of a magnetic interaction region in the body of the tube for use as opening switches by the superposition of a quenching magnetic field across the interaction region. The entire tube embraces a single plasma gaseous discharge, which conducts electron current from the hot cathode through the grid-controlling and/or interaction regions to the anode or one of a series of anode electrodes.

Work previously reported suggested that the location of the grid-controlling region relative to the interaction region had an effect on the stability of the tube during normal operation. Present work tends to confirm that location of the interaction region between the high voltage anode-grid holdoff region and the cathode decreases triggering delay and instability.

Placement of the high voltage holdoff region between the interaction and the cathode region has the disadvantages of: 1) adding an additional baffled transition region to the plasma column; 2) constructing an unnecessary

additional cavity for the plasma discharge; and 3) disturbing the optimum holdoff section geometry.

The magnetic field required for fault quenching has been determined for RSI003 to roughly obey the relation Bq (kGauss) = $0.97\ L^{-0.78}\ Ebb^{1.26}\ ib^{0.24}$. (L in cm, Ebb in KV, ib in amperes)

RSI voltage drops in the interaction region are roughly 14 volts/cm for interaction columns ranging from 14 to 80 cm.

1.3 TEST PROCEDURE

The RSI tubes were tested in the circuit as shown in Figure 1. Thyratron A is used to provide normal 6-microsecond, 20-amp pulse triggering of the RSI. Thyratron B is used to provide a 300-500 microsecond, 300-amp fault pulse to the RSI, with Rrc used to control peak current in the fault discharge. When testing for interaction region effects, the anode-grid holdoff region was either shorted or tied together with a 1 megohm resistor.

In normal pulse operation, measurements were taken of voltage drop across the RSI and observations were made of triggering delays and jitter. The effects of tube interaction length, pressure, voltage and the use of keep-alive currents were studied.

In fault interruption operation, the magnet storage capacitor was discharged after a 5-microsecond time delay from the firing of the fault current pulse. Tube pressure, interaction tube length, voltage, and current are varied to determine their effects on the magnet voltage required to interrupt the fault discharge. The peak magnetic field is directly proportional to the magnet supply voltage.

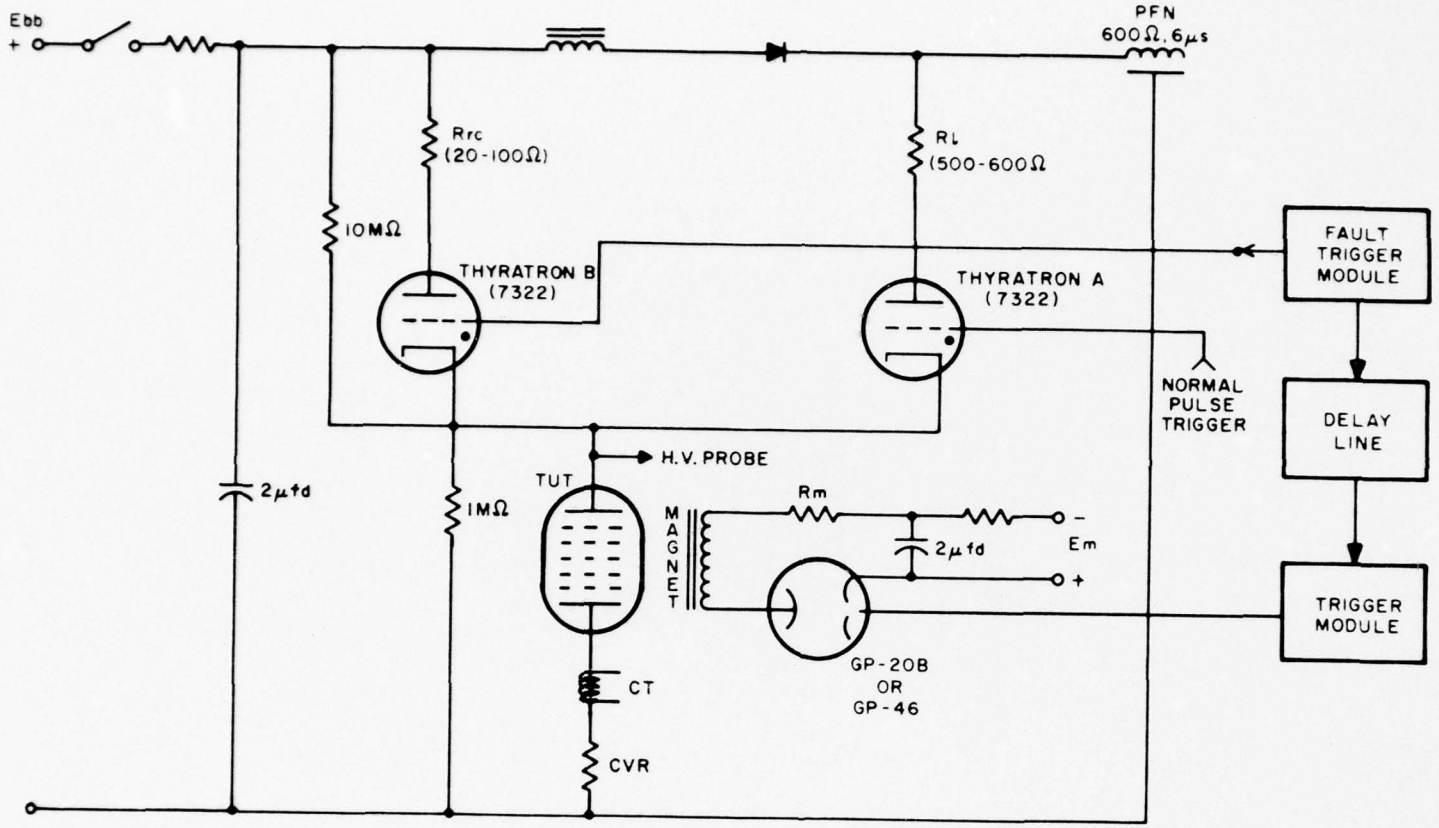

Figure 1. RSI Test Circuit.

2. CURRENT PROGRESS

2.1 TUBES UNDER STUDY

Tubes available for study during this period included the RSI 001, 002, and 003, which were described in the First Triannual Report, as well as tubes from the earlier MCCD (Magnetic-Controlled Charging Diode) contract, specifically those designated 380D-250, 400D-250, and 425H-181. Design characteristics for these tubes are given in Table 1. C-G indicates interaction region between cathode and grid; PA indicates that the interaction region is post-anode or appended to the holdoff anode.

The RSI 001 was not run during this period; data used in this report were obtained in the first study period.

The RSI 002, which gave conflicting data earlier, was subjected to re-examination. It was inferred that the probable cause of its poor operation stemmed from internal arcing at high Ebb in the thyratron body, caused by the transition from the interaction region through grid-anode space to the cathode region. In one mode of operation, internal arcing was clearly visible at the grid lead feed-through region. Data presented for this tube must be considered questionable.

The RSI 003 was the principal tube run during this period, being a compliant and versatile tube operable under a wide voltage range and what presently appears to be a remarkable pressure range. The tube developed a pressure leak after detailed study, requiring removal and, because of the nature of the tube, complete disassembly for repair. The tube will be returned to confirm possibilities of operation at low pressure. A cross section

Table 1. Tube Design Characteristics.

Tube No.	Other Designation	Number of Interaction Sections	ID (in.)	Total Interaction Length (in.)	Fill Pressure (torr)	Gas	Interaction Region Location
RSI 001		1	0.24	5.5	0.400	H_2	C-G
RSI 002		1	0.24	5.5	0.400	H_2	PA
RSI 003		5	0.375	31.75	0.400	H_2	C-G
380D-250	8131	6	0.25	23.25	0.380	D_2	PA
400D-250	MCCD 004	4	0.25	23.4	0.400	D_2	PA
425H-181	767	4	0.181	36.5	0.425	H_2	PA

of this tube is shown in Figure 2. Points A, B, C, D, and E refer to electrodes used as anodes during tests to determine the effects of length of interaction tube on operation.

The 380D-250 ran with difficulty when any portion of the interaction channel was placed in operation. Operation as a standard thyratron was satisfactory, but difficult plasma commutation through the interaction tube-first anode region caused high voltage drop, poor firing consistency, jittery operation, and extremely poor Δtad (5 to 25 microseconds); the tube required high pressure and keep-alive currents for operation. No data were taken for this tube.

The 400D-250 ran well, although it required moderately high pressure and voltage to begin operation and to stabilize pulse-to-pulse jitter. Data are presented for this tube.

The 425H-181 had external arcing problems that are presently being resolved. Some data have been taken, indicating relative advantages of thinner diameter interaction tubes.

2.2 PARAMETRIC STUDIES

The first concern during this period of study was the determination of effects of operational and design parameters on tube performance. Primary parameters for examination were: length and diameter of the interaction channel, tube voltage and peak current, and tube pressure. Additional parameters for the Pulse Forming Network (PFN) pulse study included pulse repetition rate (prr) and use of keep-alive current. For the fault-quenching study, magnetic field intensity, direction, and homogeneity are included, as well as delay time before the onset of the quenching field after fault. Of further interest (and complication) were the effects of tube geometry, fill gas, electrode size, and external circuitry.

Data obtained are separated by the effect upon tube voltage drop, quenching field, and triggering delays and jitter.

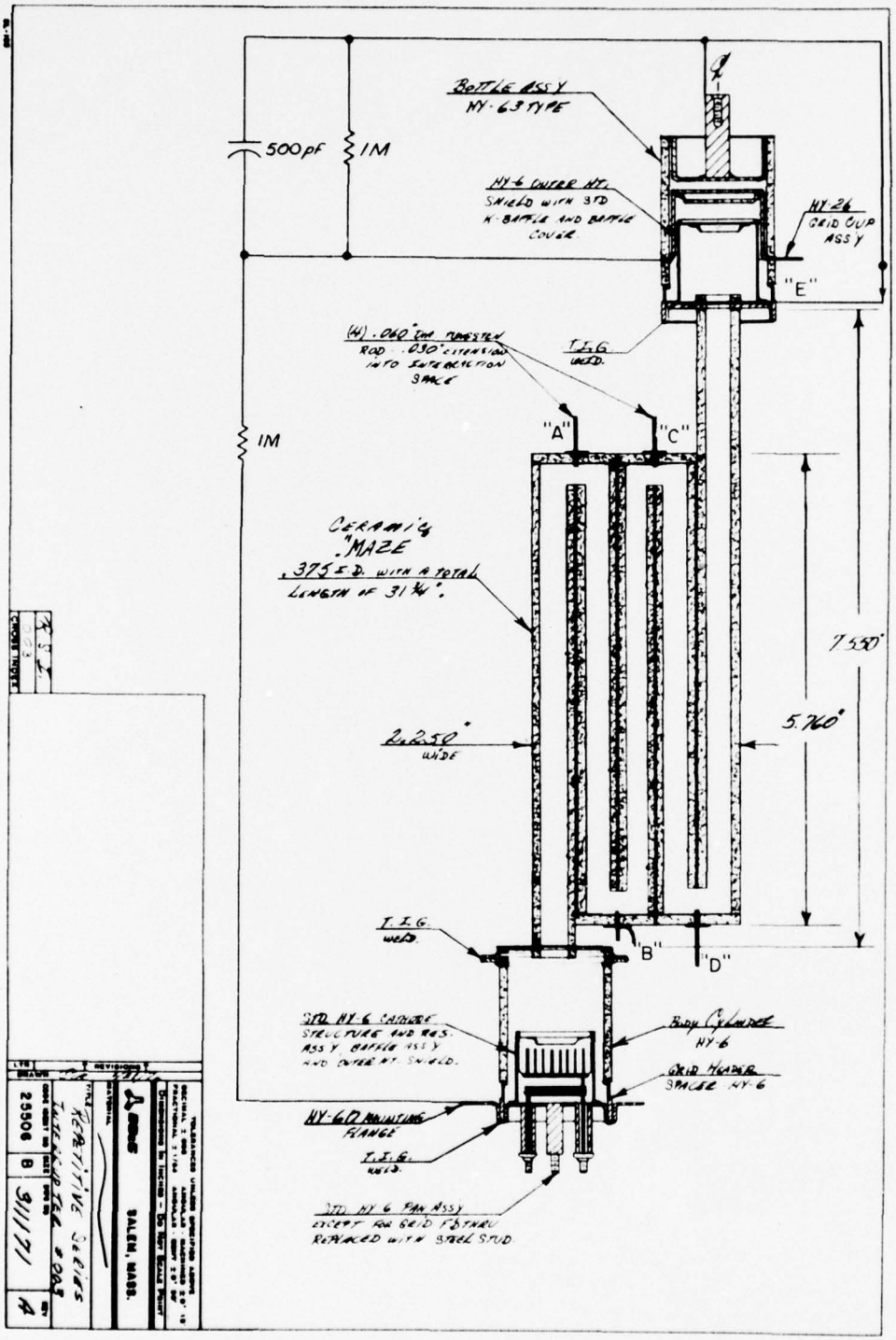

Figure 2. Tube RSI 003 and Connections.

2.2.1 RSI Voltage Drop

It has been established previously (Contract ECOM-0320-1; present contract, First Report) that voltage drop in the RSI would be a principal cause of concern during tube design. To reach contract specifications of 350 volts maximum, a short interaction tube is required, which results in extremely high quenching magnetic fields. The following parametric studies were performed to determine possible methods of improving performance.

Effects of Length

Variation of interaction channel length has the most important effect on tube voltage drop, shown in Figure 3. Data taken from multifold tubes show a near linear relationship of voltage drop to length, with voltage drop per centimeter as listed in Table 2. The moderate nonlinearities at the extremes of the curves in Figure 3 are the result of additional anode and cathode drops in the thyratron sections of the tube, and do not conflict with linearity of the interaction region data.

Effects of Diameter

Data from several tubes are summarized in Table 2, showing an increase in tube drop with decreasing tube diameter. Available data only provide a general trend; however, it appears that tube drop does not increase markedly until an internal diameter of less than 0.25 inch is used.

An experimental and theoretical study (Brown, 1959) of voltage drops in discharge tubes is shown in Figure 4 together with latest data. It is seen that there is some agreement with previous data, although the presently obtained values appear to be somewhat less than extrapolations of earlier curves. The curves are plotted as voltage drop per centimeter per pressure (torr) $\frac{E}{P}$ versus the parameter rp (tube radius times tube pressure).

Table 2. Voltage Drops of Multifold Tubes.

Tube No.	ID (in.)	Eres (volt)	P (torr) (calculated)	Tube Drop E (volt/cm)	$\frac{E}{P}$ $\frac{\text{volt}}{\text{cm-torr}}$	rp (cm-torr)
RSI 003	0.375	4.0		11.8		
		5.6	0.30	13.8	46.8	0.141
		6.0	0.36	14.1	39.7	0.169
		6.6	0.45	15.7	35.3	0.212
		7.2	0.54	19.0	35.5	0.255
RSI 001	0.24	5.6	0.30	13.6	46.1	0.09
		6.4	0.42	16.4	39.5	0.13
		7.2	0.54	18.6	34.8	0.16
MCCD 400D-250	0.25	7.0	0.51	15.9	31.5	0.063
MCCD 425H-181	0.181	5.6	0.32	21.5	67.2	0.08

A possible explanation for the disagreement is that at low "rp" as is present in our tubes, wall effects become more important than gaseous interaction effects in the generation of the plasma column electric field. It is suspected that unique functional dependence upon the rp parameter breaks down at low numbers and that differing curves represent this divergence.

Effects of Current

Because of impedance mismatching between the PFN (600 ohms) and R1, no high prr tests could be made with low R1. Tests performed at low prr showed that changing R1, and hence changing the current during conduction, had no visible effect on the voltage drop in the tube. However, the pulse forming network is currently limited to about 20 amperes peak. An examination of RC fault conduction at the 20-30 amp level indicates that there may be a slight improvement in RSI voltage drop at a higher PFN current level.

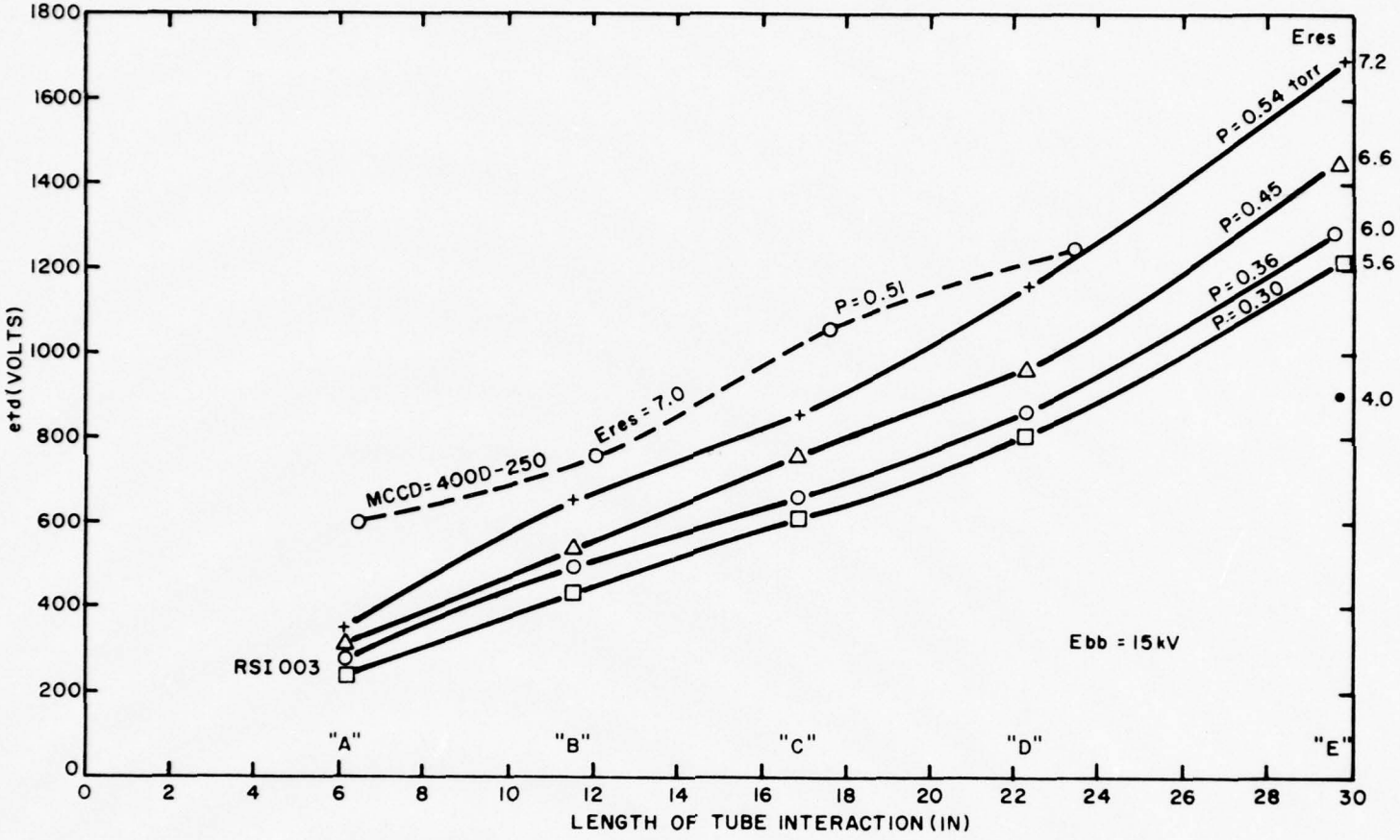

Figure 3. Voltage Drop Versus Length and Pressure.

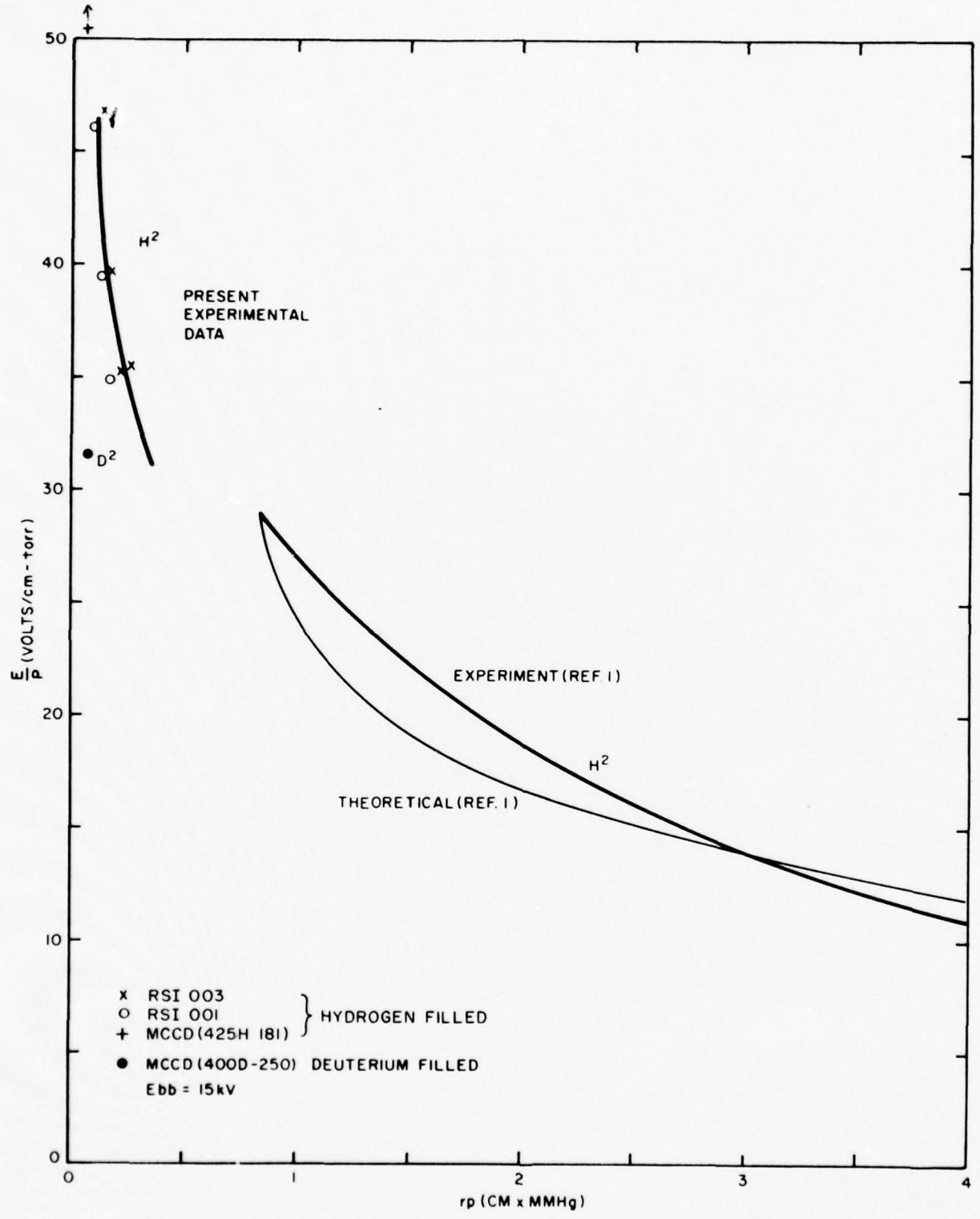

Figure 4. Comparison of Present and Previous Tube Voltage Drops (Experimental and Theoretical).

Effects of Keep-Alive Current

Keep-alive currents were utilized in the study of the RSI 003 under a variety of conditions, including variation of electrodes used, length of conduction path, tube pressure, and tube voltage. No evidence was seen that the addition of the keep-alive to the tube had any effect on either current or voltage waveforms other than to alter their triggering and delay characteristics.

Effects of Pressure

Figure 3 also shows the effect of pressure on voltage drop for the RSI 003. More than 10% voltage reduction is gained by reducing Eres from the 6.3-volt standard (0.400 torr) to 5.6 volts (0.295 torr). However, a reduction of 35% is realized when Eres is reduced to 4.0, which may be below stable operable conditions.

Previously reported data for the RSI 001 showed roughly equivalent data.

The MCCD 400D-250 likewise revealed a similar decrease, although firing difficulties below an Eres of 6.5 precluded getting adequate data.

Effects of Pulse Repetition Rate

It was observed that changes in prr had little effect on tube waveforms. Several tubes, however, failed to fire at a 300-2000 pulse per second repetition rate at moderate to low pressure, or they would fire erratically. A possible cause for this behavior is gas depletion, which could have a major influence on tube operation.

2.2.2 Magnetic Field for Current Interruption

The other consideration in RSI tube design is the level of magnetic field required to successfully interrupt the fault discharge. EG&G's present experiment utilizes a magnetic core with an airgap within which the RSI tube is placed for crossed-field quenching. Five turns of wire on the core provide magnetic induction when pulsed from a series RC circuit.

Contract specifications aim toward interruption field energy of 50 joules per pulse. Taken as a uniform field over the full RSI 003 tube volume of 2 by 5.5 by 0.5 inches (90 cubic centimeters), this energy level corresponds to a field of 11.8 kilogauss, neglecting fringe and core losses. However, actual operation requires considerably higher energy in capacitor storage (550 joules at present for the same field) for the generation of that field. Energy requirements may be reduced by alteration of tube volume, core size and shape, RLC circuitry, and energy-switching techniques, so that final energy consumption will fall somewhere between the above values. Present experiments indicate quenching of a 15-kilovolt, 300-ampere pulse with a 5.9 kilogauss field (31 to 140 joules).

In the following parametric studies, the quenching field is taken as that level of field required to reduce tube current to zero at some instant of time, and not necessarily (and not usually) to hold it off once quenched. With some tubes, it is taken as that point at which the tube quenches 50% of the time. This data definition was chosen as an observable and comparable reference point, and differs slightly (but not markedly) from 100% quenching.

Several runs were taken varying both tube length and load resistance (and therefore tube current) for the RSI 003 during quenching as shown, for instance, in Figure 5 (point C data have been removed for clarity). Since variation of Ebb produces variation in both quenched voltage and tube current, the two effects were separated by plotting constant current and constant voltage points (interpolated from obtained data) on log-log graphs as shown in Figure 6, and taking slopes from these curves to indicate the exponential dependencies of these parameters.

Effects of Length

The effect of interaction channel length upon quenching field appears to be a function of both tube voltage and tube current. Two separate experimental runs produced the values given in Tables 3 and 4, where the only difference between runs was the direction of the magnetic field, as indicated. The numbers given refer to the values of m for the equation: $Bq \propto L^{-m}$.

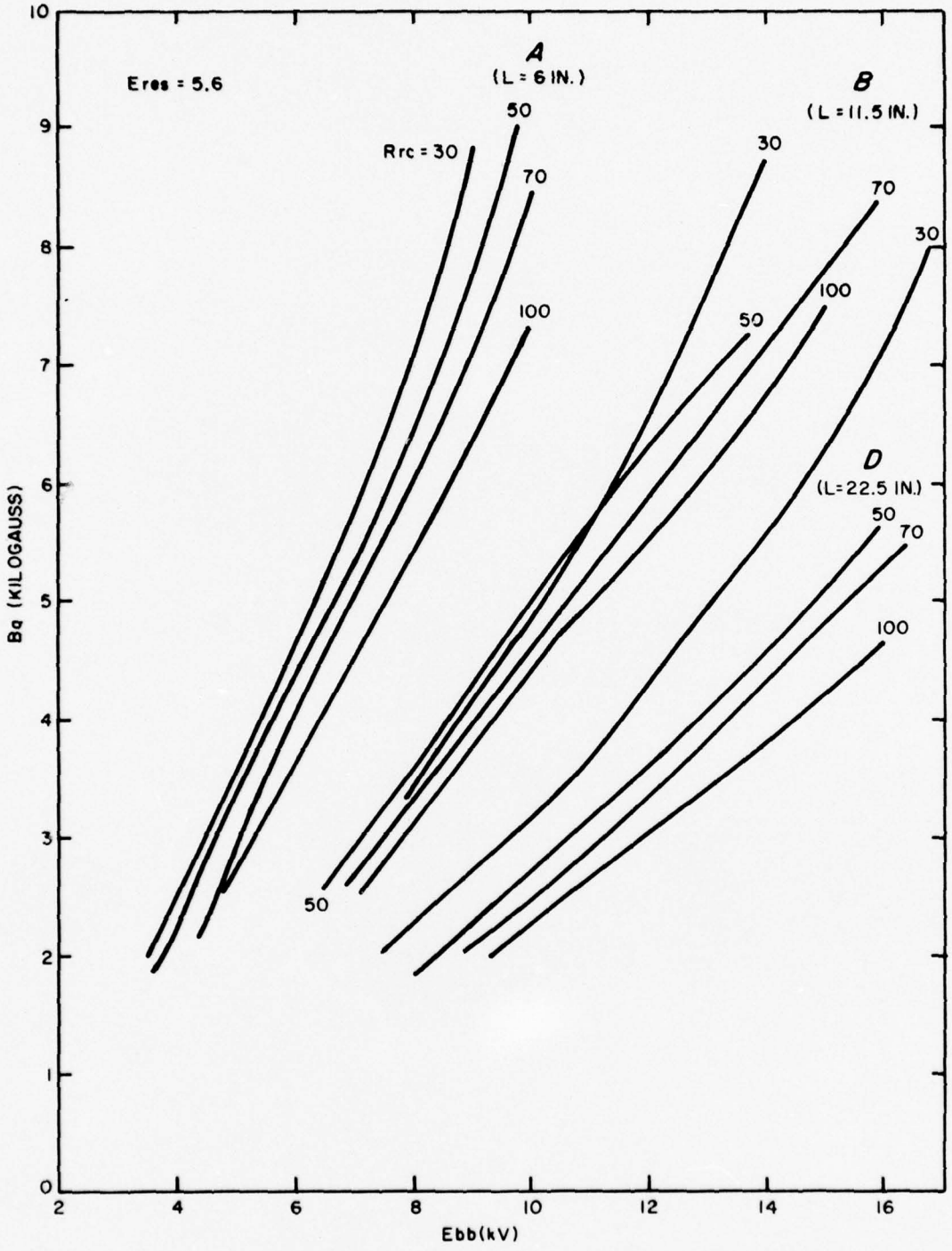

Figure 5. Quenching Magnetic Field Versus RSI Supply Voltage (Ebb), Length of Interaction Tube (L), and the Fault Network Load Resistance (Rrc) for the RSI 003.

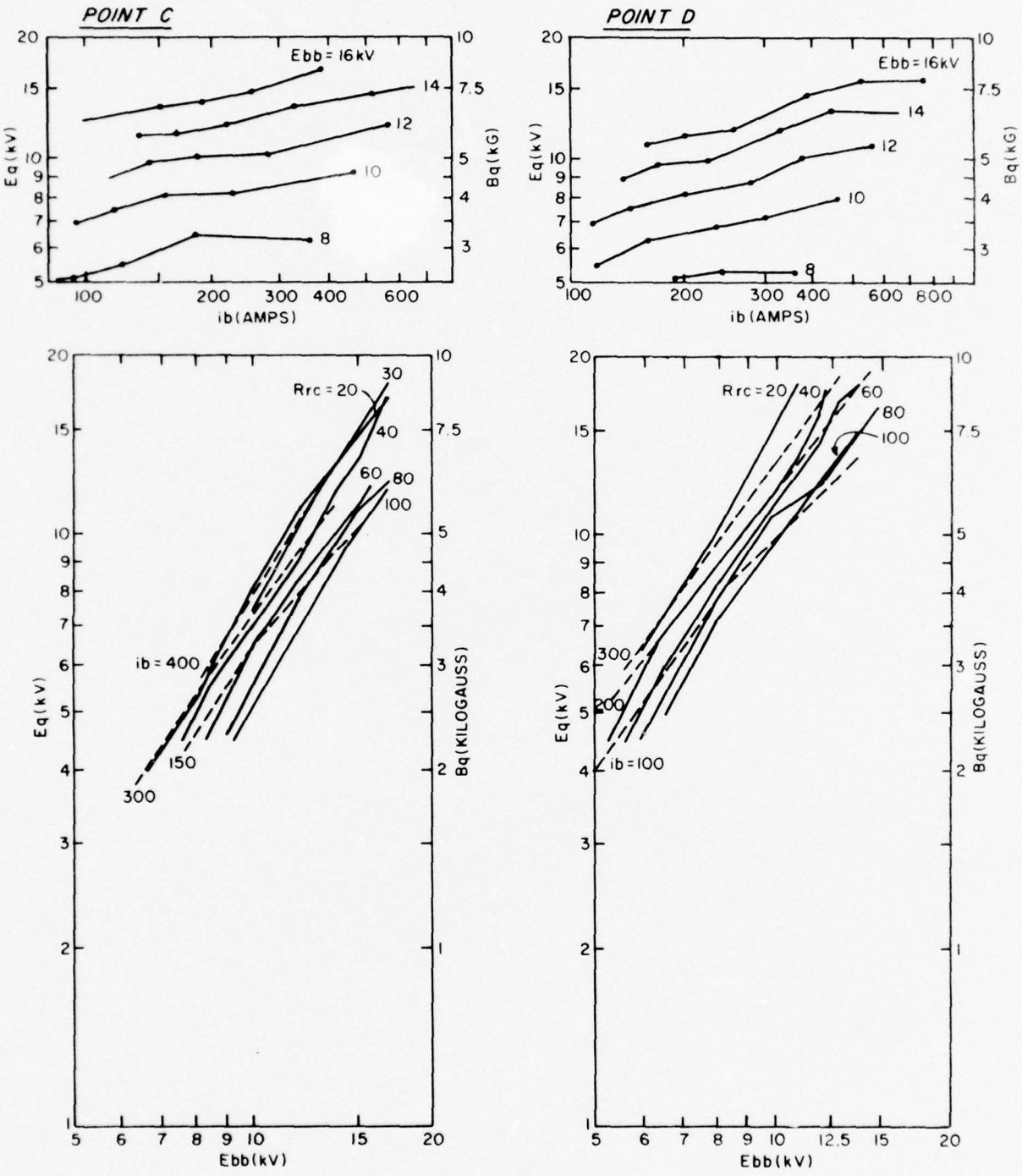

Figure 6. Quenching Magnetic Field (Bq) Versus Peak RSI-Current (ib) and Voltage (Ebb): Separation of Parameters in the RSI 003. (Eres = 5.6)

Table 3. Values of m for Bq $\propto L^{-m}$ for RSI 003.

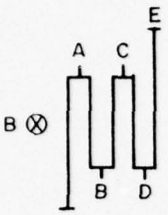

FIELD DIRECTION

ib (amperes)	Ebb (kilovolts) ⟶				
	8	10	12	14	16
100	0.90	0.92	0.74	—	—
150	0.83	0.74	0.69	0.59	—
200	0.73	0.65	0.73	0.70	—
250	0.76	0.77	0.77	0.74	—
300	0.76	0.68	0.81	—	—
400	0.76	0.83	—	—	—

Table 4. Values of m for Bq $\propto L^{-m}$ for RSI 003.

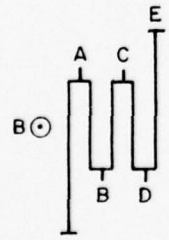

FIELD DIRECTION

ib (amperes)	Ebb (kilovolts) ⟶				
	8	10	12	14	16
100	0.93	0.89	0.88	0.87	—
150	0.91	0.89	—	0.87	—
200	0.87	—	0.90	—	0.68
250	—	0.76	0.76	0.87	—
300	0.83	0.68	0.77	0.62	—
350	—	—	0.63	—	—
400	—	—	—	0.71	—

Some of the graphs from which these data were taken are given in Figure 7, where each curve represents a particular voltage and current combination. The limited number of points for each curve explains the scattering of data values for m in Tables 3 and 4, but does not explain the trend of the data. Points for these curves have been shifted slightly to take into account the presumed difference of plasma conduction path lengths with field direction. This occurs because the plasma column is folded, and the plasma discharge is forced to either the inner or the outer wall at the folds depending upon field direction. It has been noticed that correcting for this shift somewhat improves linearity of the data on the log-log plots.

The data for low currents and voltages are in agreement with earlier work (Thomas, 1967) which concluded that m be approximately 1. The fact that m decreases at high power is discouraging, since it means that the discharge becomes harder to quench under these conditions.

Effects of Diameter

Decreasing the tube diameter causes a marked decrease in the magnetic field required for quenching. Figure 8 shows quenching curves for two smaller diameter tubes, as compared with Figures 5 and 12 for RSI 003. When allowances are made for the different pressures and lengths at which these tubes were run, it then appears that the 0.25-inch inside diameter tube is only slightly easier to quench than the 0.375-inch inside diameter tube, and that the 0.181-inch inside diameter tube represents a significant change in reducing the required field. More data are needed before a generalization is made, but inside diameters within the range of 0.25 to 0.375 inches may be preferable.

Effects of Current and Voltage

As previously indicated, voltage and current effects are interdependent but separable. Data from curves such as Figure 6 were used to calculate the exponents of the equation: $Bq \propto (Ebb)^{\beta} (ib)^{\delta}$. Experimental values are given in Tables 5 and 6. The data are somewhat erratic and trends are not apparent.

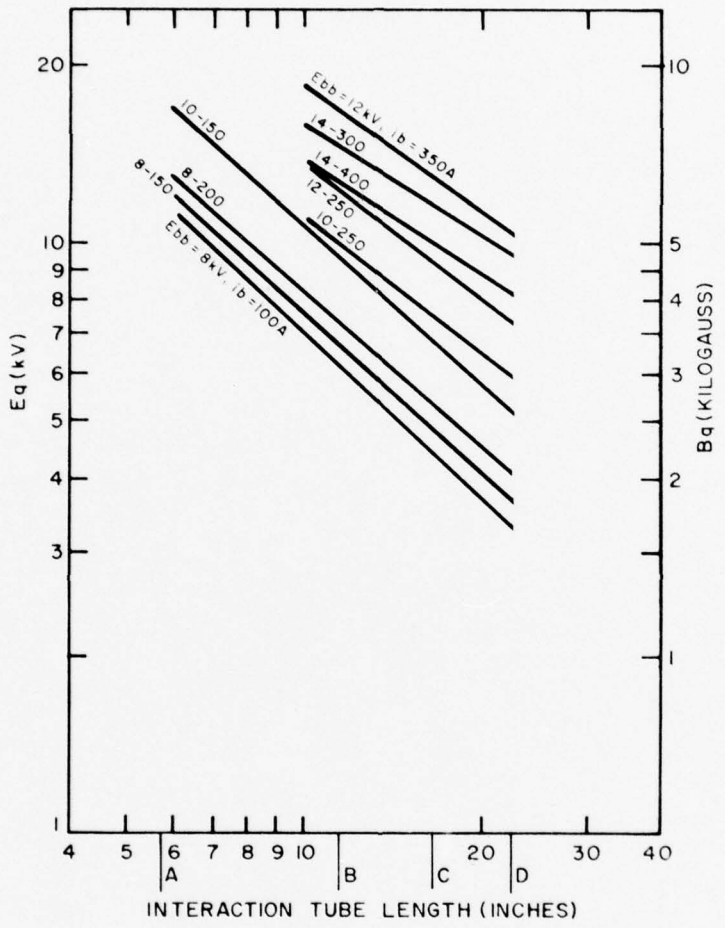

Figure 7. Quenching Magnetic Field Versus Tube Length, Main Supply Voltage (Ebb) and Peak-RSI-Carried Current (ib) for the RSI 003.

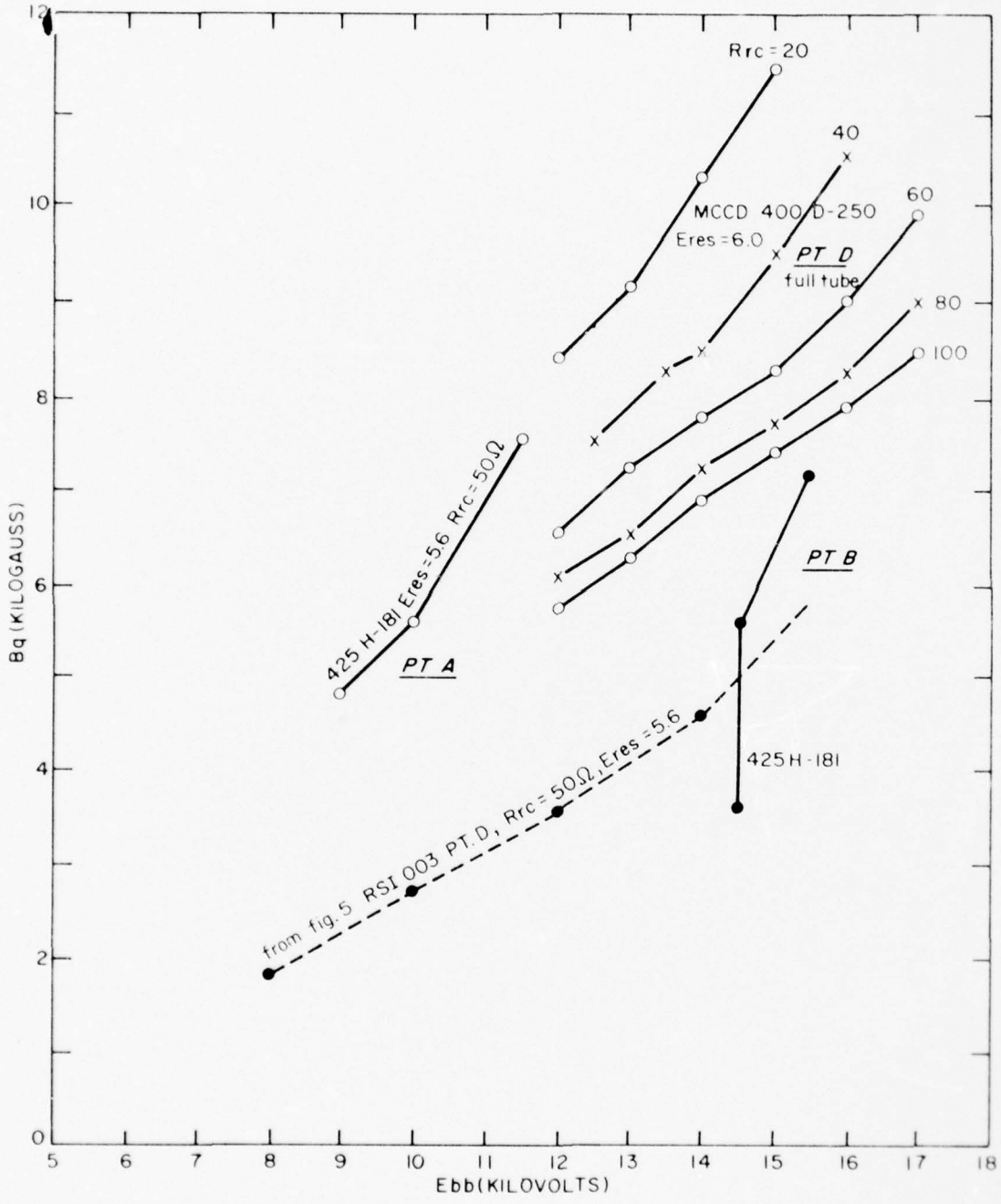

Figure 8. Quenching Field Versus Main Supply Voltage (Ebb) for Several Tubes.

Table 5. Experimental Values of β for the Equation Bq α (Ebb)$^{\beta}$. RSI 003 Eres = 5.6.

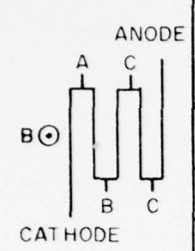

Anode Point	Peak RSI Current, ib (Amperes)						
	50	100	150	200	250	300	400
A	1.22	1.16	–	–	–	–	–
B	–	1.25	–	1.25	–	–	–
C	–	1.21	–	1.30	1.32	–	–
D	–	1.41	–	1.21	–	–	–

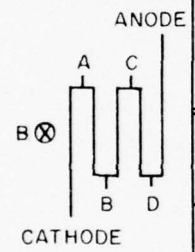

Anode Point	Peak RSI Current, ib (Amperes)						
	50	100	150	200	250	300	400
A	← 1.41 (Fringe Field) →						
B	–	1.28	1.05	1.19	–	1.25	–
C	–	1.26	1.10	1.15	–	1.28	1.32
D	–	1.47	–	–	–	1.32	1.43

Table 6. Experimental Values for δ for the Equation Bq α $(Eb)^{\delta}$. RSI 003 Eres = 5.6.

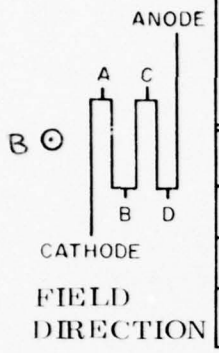

Anode Point	Main Supply Voltage, Ebb (Kilovolts)								
	5	6	7	8	10	12	14	15	16
A	–	0.18	–	0.43	0.57	–	–	–	–
B	–	–	–	0.24	0.06	0.19	–	0.17	–
C	–	–	–	0.42	0.21	0.25	–	0.31	–
D	–	–	–	0.47	0.44	0.30	–	0.34	–

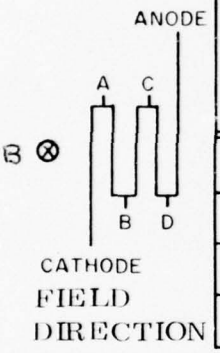

Anode Point	Main Supply Voltage, Ebb (Kilovolts)								
	5	6	7	8	10	12	14	15	16
A	0.04	0.02	0.04	0.07	–	–	–	–	–
B	–	–	–	0.17	0.22	0.30	0.30	–	–
C	–	–	–	0.14	0.14	0.14	0.18	–	0.19
D	–	–	–	0.06	0.28	0.31	0.32	–	0.31

Effects of Pressure

Pressure has a substantial effect on quenching requirements, particularly at higher voltages, as is evident in Figure 9. Experiments at lower pressure, though incomplete, indicate that continued improvement in required field levels occurs with progressively lower pressure; one point taken for the RSI 003 at very low pressure is added to demonstrate this fact. Figure 10 shows similar data for the MCCD 400D-250.

Effects of Magnet Firing Delay

The delay imposed on the circuit between the start of thyratron conduction and magnet discharge (τ_D) has the effect for magnetic quenching field shown in Figure 11. The graph represents a magnetic field which peaks after approximately 9 microseconds. The fault current itself reaches maximum after about 1 microsecond. The curve presented seems to indicate that the fault-inspired tube plasma is easiest to extinguish early in an 11-microsecond period which the plasma requires to achieve maximum ionization. A fast rise time magnet current is therefore indicated.

Effects of Magnetic Field Shape

No specific work was performed in this regard except for a study of the effects of fringe fields at the borders of the core gap. Figure 12 shows the effect of shifting the RSI away from the fringe fields (shaded area) at the interaction regions nearest the cathode. As would be expected, the discharge becomes easier to quench when all or part of the plasma column is farther within the full-field region of the magnet gap. An unexpected result obtained from a different experimental run indicated that a plasma column subjected entirely to a fringe field could be quenched with an equal but high field, independent of tube current (for the same tube voltage).

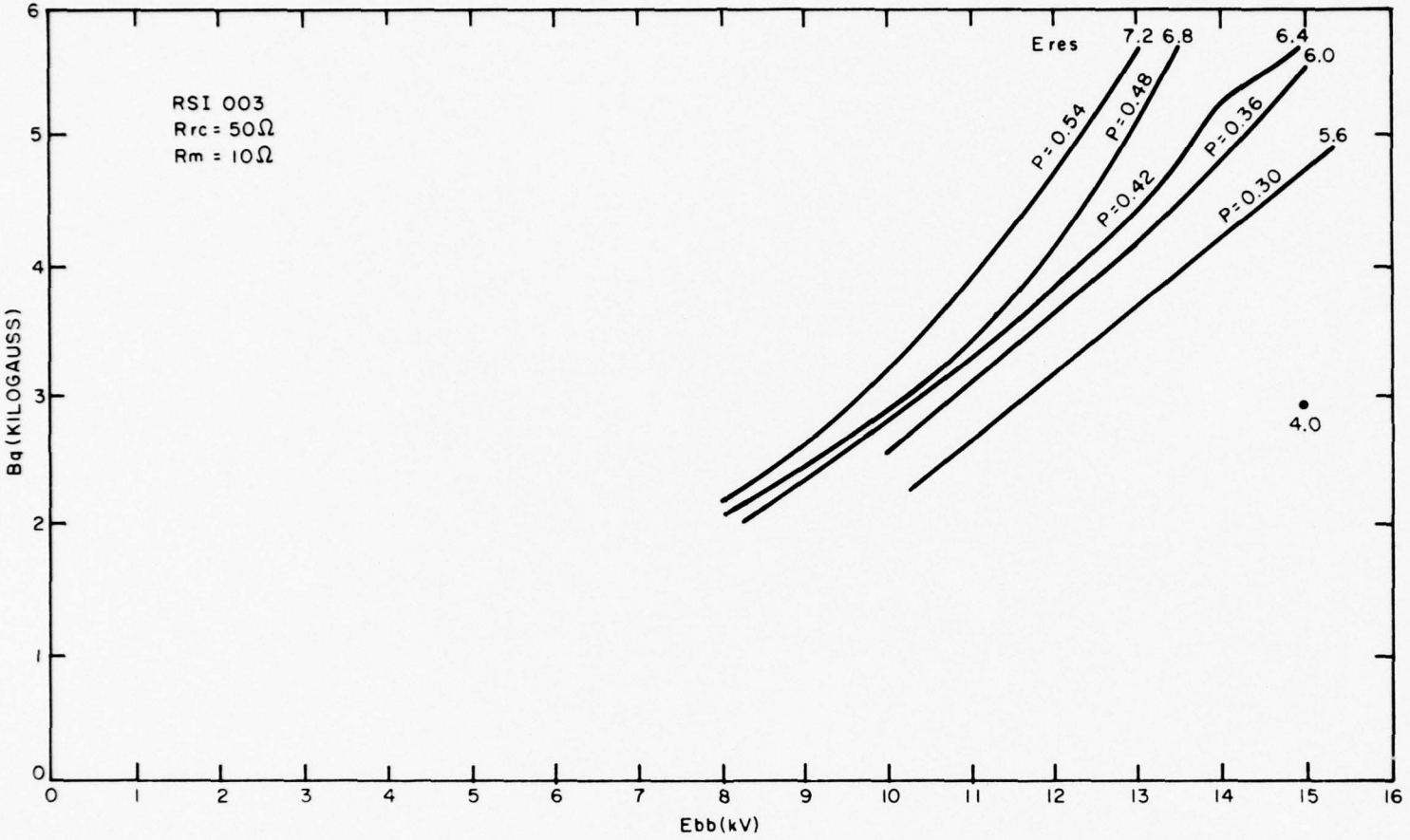

Figure 9. Quenching Field Versus Main Supply Voltage (Ebb) and Pressure (P) for the RSI 003.

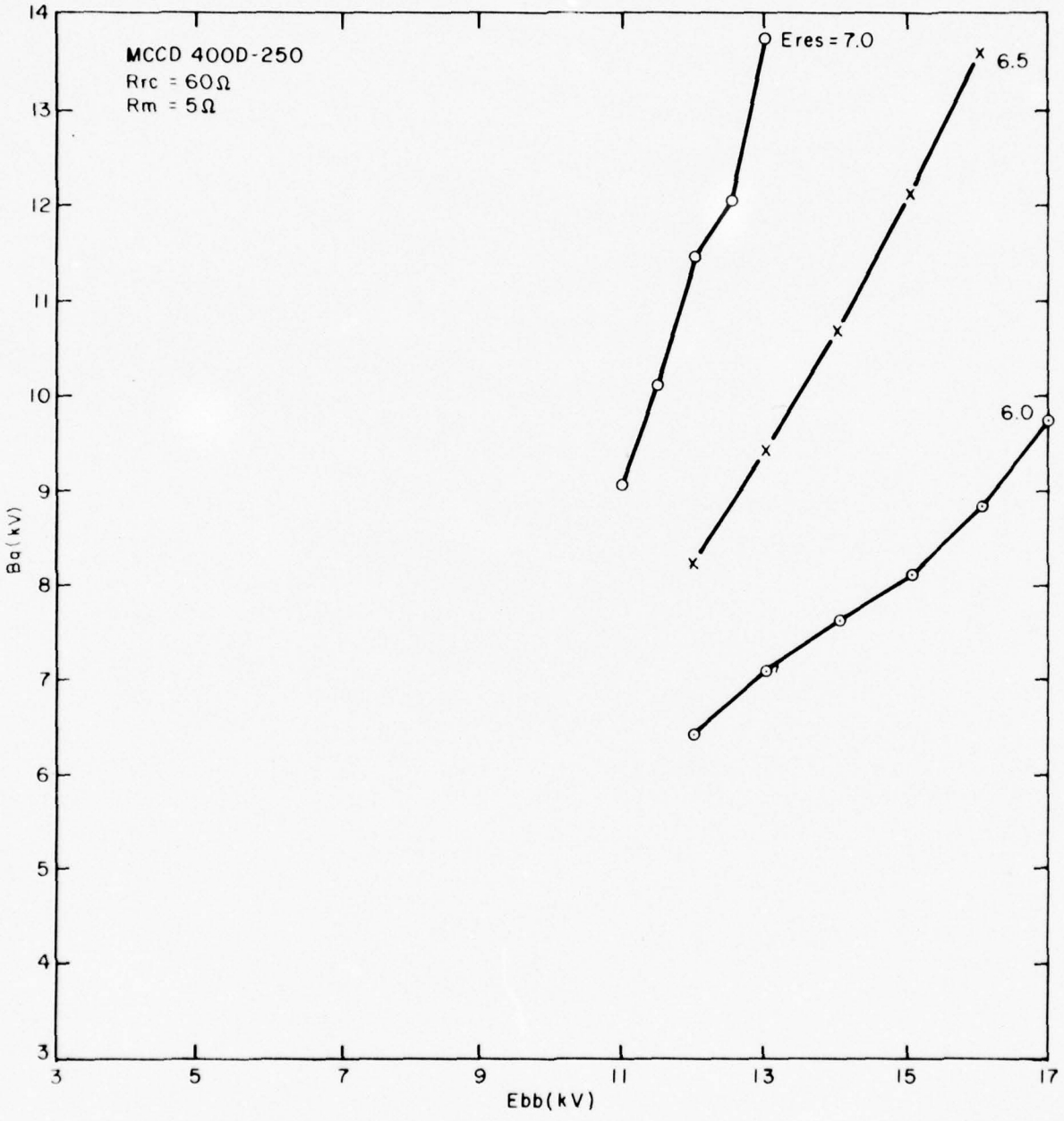

Figure 10. Quenching Field Versus Main Supply Voltage (Ebb) for the MCCD 400D-250.

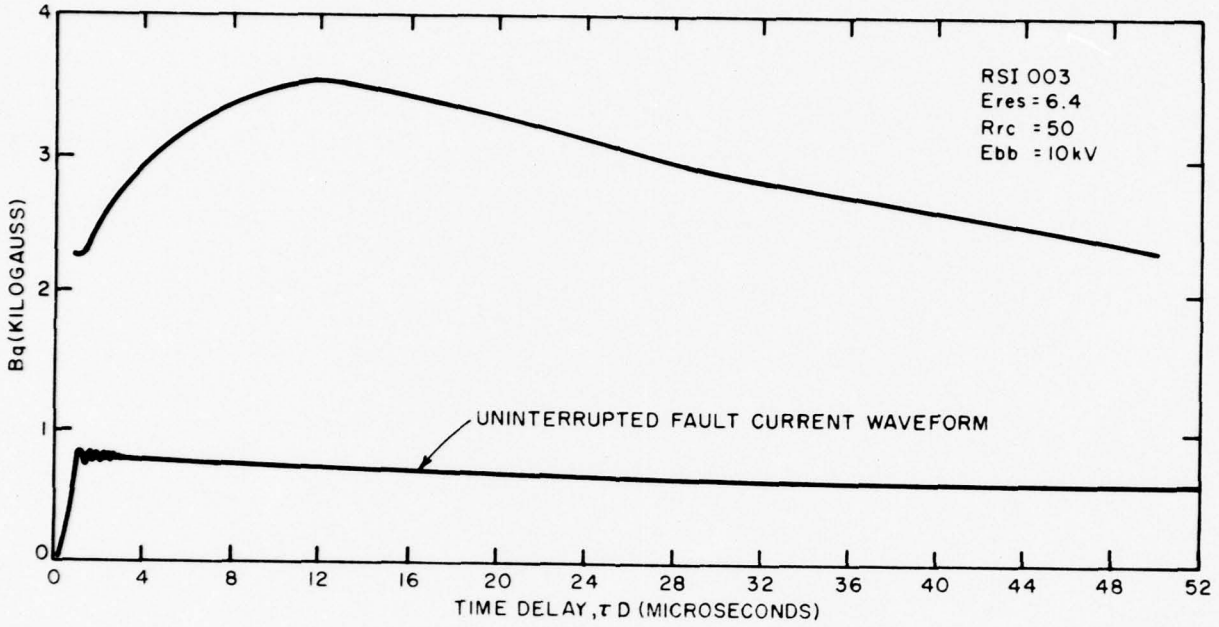

Figure 11. Quenching Field Versus Magnetic Circuit Firing Delay for the RSI 003.

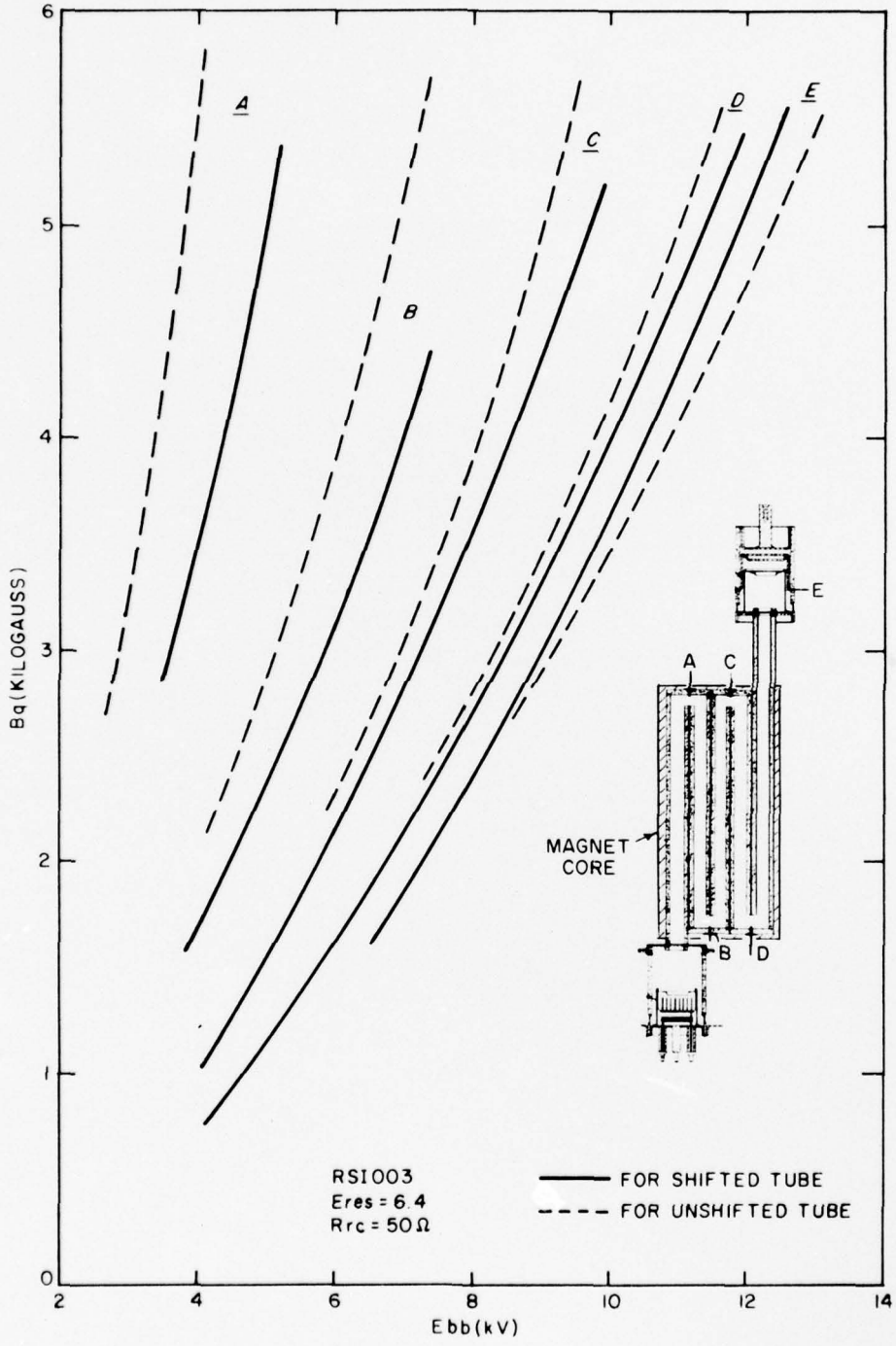

Figure 12. Average Quenching Field [1/2 (B ⊗ + B ⊙)] for the RSI 003.

Quenching Mechanism

Empirical studies indicate that there may be more than one mechanism associated with quenching behavior, or at least that there is a transition between two related modes of current interruption.

When the critical quenching magnetic field is approached by increasing the magnetic field from pulse to pulse, two different effects are noticed. In one mechanism, shown in Figure 13a, the tube current slowly decreases until the point is reached at which it is effectively zero. In the other mechanism, Figure 13b, the current decreases to a point, but then a slight increase in field results in a sudden quench. Occasional rapid and noisy oscillations can be seen at this point, particularly on the voltage waveform. No explanation has yet been proposed for this phenomenon, nor has a study been done to determine the parameters of transition between mechanisms.

Effects of Field Direction

First experiments suggested that there might be a preferred field direction for fault quenching. A study of this effect demonstrated that the probable cause for observed discrepancies was due to fringe-field quenching rather than field direction.

2.2.3 Triggering, Delay, and Jitter Characteristics

For the greater part of these investigations, the RSI tube under study has been connected with a 7322 thyratron in series. The RSI was run with its holdoff region externally short-circuited or bypassed, and the 7322 was used to hold off and trigger the circuit. The reason for this was to isolate the interaction section of the tube for a particular study.

Pulse-delay measurements were made, particularly with regard to the use of a keep-alive current between combinations of cathode and A, B, C, D electrodes in the full tube RSI 003. Delays measured ranged from 0.8 to 1.9 microseconds, with smallest delays occurring for high voltages, but were generally independent of pressure. Keep-alive currents reduced delays

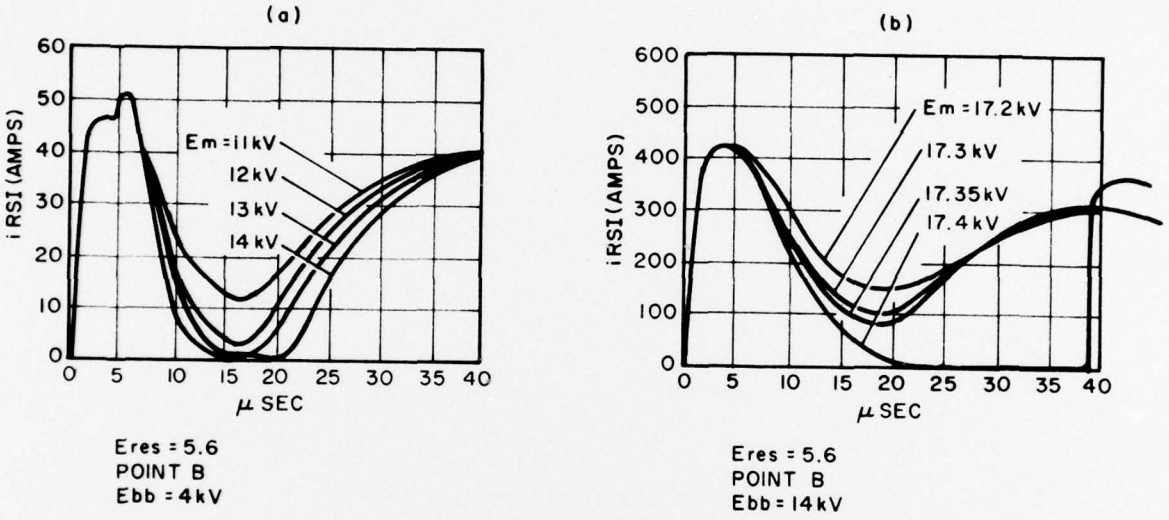

Figure 13. Fault Current Interruption for RSI 003.

to 0.450 to 1.6 microseconds and were also independent of pressure. Keep-alive currents used for this purpose were of the order of a few milliamperes; keep-alive voltages were from 2 to 10 kilovolts.

Pulse-to-pulse jitter was watched only briefly during this period of investigation, again chiefly with regard to the use of keep-alive currents. The MCCD 400D-250 gave total pulse jitter and a Δtad of up to several hundred nanoseconds, with improvement at high pressure and high voltage to under 10 nanoseconds (limit of resolution). Keep-alive currents had differing effects upon tube jitter, as both improvements and degradations were noted. The RSI 003 was considerably more jitter free than the MCCD tube, but no values were taken for comparison.

Generally, decreasing pressure has the effect of increasing pulse-to-pulse jitter. It will be important, considering the effect of low pressure on tube drop and quenching field, to determine how best to reduce low pressure jitter. Present investigations suggest that use of a virtual anode or anode cavity improve RSI stability, possibly by a reduction of plasma depletion. Up until now, RSI tubes have been run with heater and reservoir voltages connected to the same power supply. It may be possible to improve low pressure stability with two isolated and separately adjustable circuits.

3. DISCUSSION OF DATA

Data taken to date suggest that the basic trade-off in RSI tube design will occur between the voltage drop and the quenching field, with considerations given next to high repetition rate and pulse and triggering stability. The parameters of tube length and diameter are critical here, as shown in Figures 14 and 15.

It has been observed for the RSI 003 that the field energy for quenching a 15-kilovolt, 270-ampere fault discharge is nearly independent of the length of the interaction tube. This result occurs since the required field increases with decreasing length, but the magnetic-field volume decreases, and the product of the two is roughly constant. However, this effect is not seen in the 425H-181 tube, and the data for the other tubes (particularly 400D-250) are not complete.

Figure 14 data of Bq versus etd are important in our present experiment because of the magnetic saturation limit of the core. A small-diameter core gap, and hence interaction region, is unusable because a high-field requirement saturates the iron core despite what might be a low field energy.

Stability under high repetition rate firing is not a simple matter, and must be assured. Pressure must be kept moderately high to allow stable tube operation, yet should be kept low for minimum voltage drop and magnetic field.

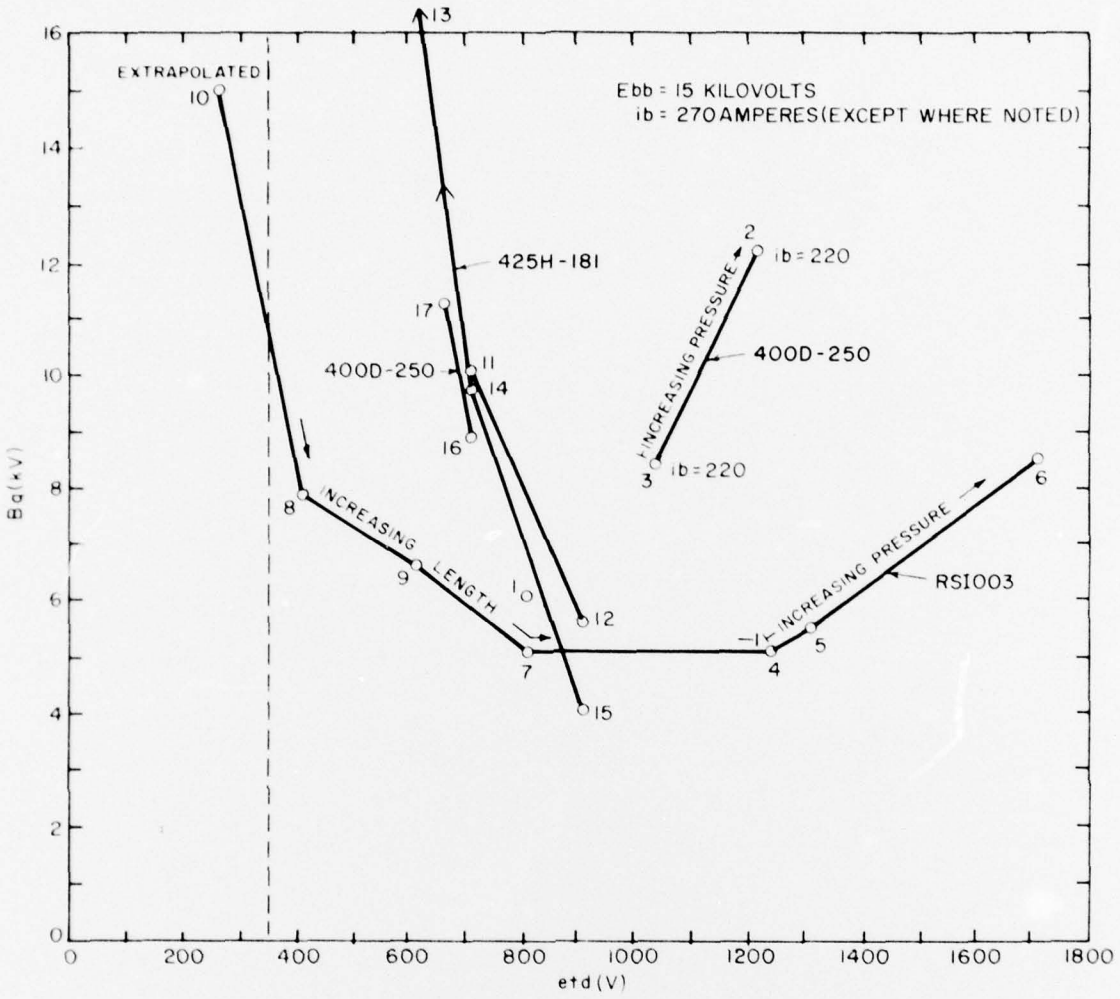

No.	Tube	Eres	Electrode Anode	Interaction Length (in)
1	425H-181	5.6	B	12.0
2	400D-250	6.5	D	23.4
3	400D-250	6.0	D	23.4
4	RSI 3	5.6	E	31.75
5	RSI 3	6.0	E	31.75
6	RSI 3	7.2	E	31.75 (Extrapolated)
7	RSI 3	5.6	D	23.0
8	RSI 3	5.6	B	11.5
9	RSI 3	5.6	C	17.3
10	RSI 3	5.6	A	5.8 (Extrapolated)
11	425H-181	5.6	B	12.0
12	425H-181	5.6	C	17.5
13	425H-181	5.6	A	6.5 Off scale for Bq
14	425H-181	5.2	B	12.0
15	425H-181	5.2	C	17.5
16	400D-250	6.0	D	23.4
17	425H-181	6.0	C	17.5

Figure 14. Quenching Field Strength Versus Tube Voltage Drop for Several Tubes.

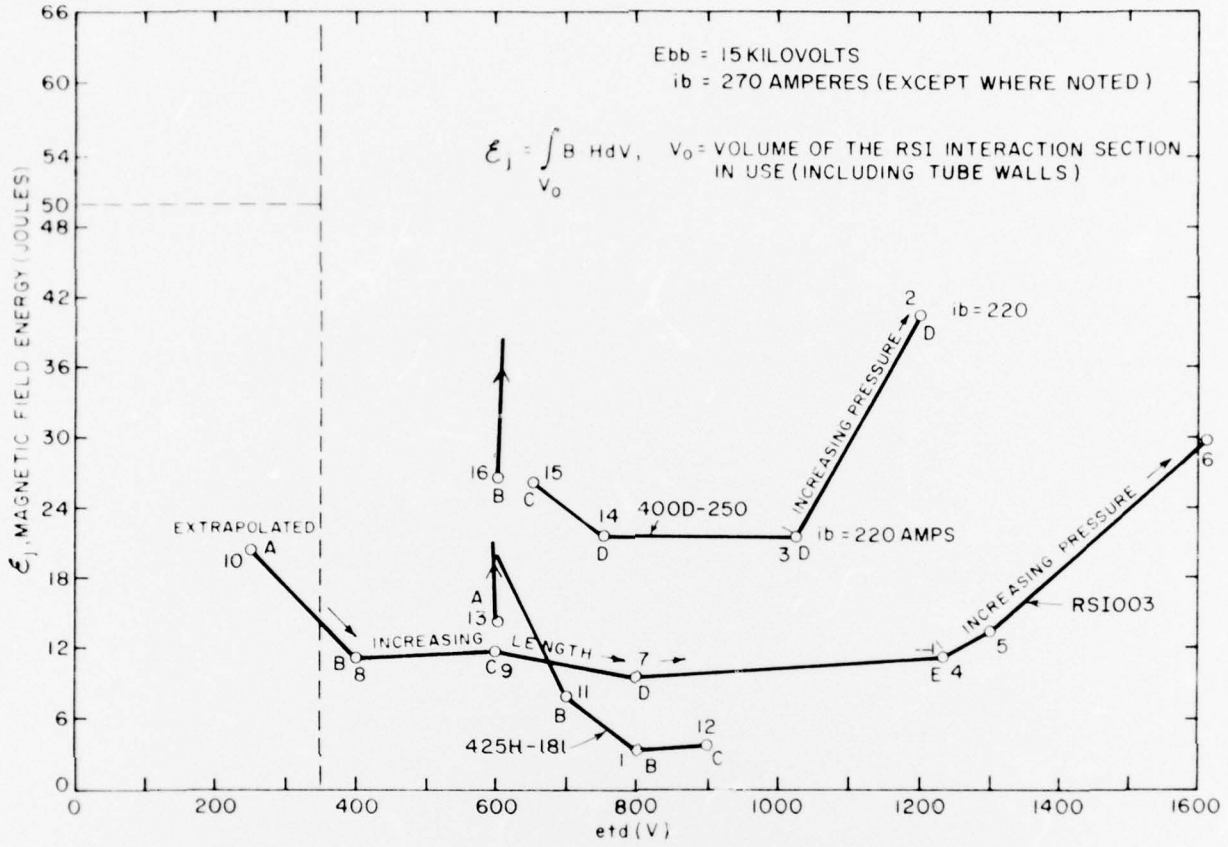

No.	Tube	Eres	Electrode Anode	Interaction Length (in)
1	425H-181	5.6	B	12.0
2	400D-250	6.5	D	23.4
3	400D-250	6.0	D	23.4
4	RSI 3	5.6	E	31.75
5	RSI 3	6.0	E	31.75
6	RSI 3	7.2	E	31.75
7	RSI 3	5.6	D	23.0
8	RSI 3	5.6	B	11.5
9	RSI 3	5.6	C	17.3
10	RSI 3 (Extrapolated)	5.6	A	5.8
11	425H-181	5.6	B	12.0
12	425H-181	5.6	C	17.5
13	425H-181	5.6	A	6.5
14	400D-250	6.0	D	23.4
15	400D-250	6.0	C	17.5
16	400D-250	6.0	B	12.0

Figure 15. Quenching Field Energy Versus Tube Voltage Drop for Several Tubes.

Extrapolation of present results to higher voltages offers advantages as well as disadvantages, since quenching becomes ever more difficult, suggesting that tube design be based on final voltage rating to a substantial degree. A working system at higher voltages appears attainable, with the major drawback being that magnetic quenching capacitor energies may be in the kilojoule range, unless some of the suggested operational improvements prove valid.

4. EXPERIMENTAL MODIFICATIONS

Minor changes have been made in the experimental setup to improve data accuracy, noise reduction, and the facility (and safety) of data collection. The basic circuit (Figure 1) is unchanged.

Magnet triggering circuitry was modified by the inclusion of a second spark gap and a change of the spark gap triggering mode. An EG&G GP-20B spark gap was added in parallel to the present GP-46 such that the former would be used for Eq from 4 to 10 kilovolts and the latter from 10 to 20 kilovolts, with some overlap, allowing for investigations of quenching trends to lower voltages. Triggering was changed to Mode A (positive trigger pulse to positive adjacent electrode) with a gain in triggering jitter stability with a slight increase in triggering delay. The quenching pulse variable delay line was re-added to the circuit, and set at 5 microseconds for most experiments. This delay value was chosen to represent an expected worst case for the electronic delay of fault sensing circuits.

Spark gap prefire, a problem with the use of a delay line, was markedly reduced by the use of noise prevention measures. Steel shielding was added around the delay line and the spark gap trigger module, and along the delay line power cord. A voltage regulator and balun were added to the power cords of the above. RF chokes were placed on trigger connections, and shielded cable was installed for the trigger signal.

Pearson current transformers (1% maximum error) have been used in addition to the precision current viewing resistor for current measurements in both TUT and magnet circuits. A 7633 Tektronix storage oscilloscope was

purchased and is in use for study of fast, single-shot quenching waveforms. A small 20-kilovolt supply with 30-milliampere capability was built for use as temporary replacement for one or two adjustable range UVC high voltage supplies (also required for other applications).

A charging switch was added in series with the TUT power supply as a means of cutting power to the TUT circuit during RC high current pulses without shutting down (and consequently resetting) the TUT supply. This is necessary at high voltages to prevent keep-alive current from flowing through the entire TUT circuit from the TUT supply. Obviously, this occurs only when the TUT has not been completely quenched.

The RSI filament and reservoir voltage supply was relocated to be visually accessible at all times during experiments. A voltage regulator was placed on its line cord to eliminate pressure fluctuations caused by line voltage fluctuations.

The quenching magnet core was repositioned and now enables the RSI tube to be optically addressed by the proposed optical measurement devices. The change also allows greater flexibility in positioning RSI tubes within the magnetic field, and is adaptable to all sizes of tube and thyratron bases. In addition, two clamp-on additions to the core were made from transformer steel to allow for increasing the magnetic interaction volume for the effective study of RSI tubes with widths greater than 2 inches. Tests indicate that the additions perform well, and comparison of relative permeabilities suggests that the enhanced field is fairly uniform below 10 kilogauss.

5. CONTINUING STUDIES

Several data gaps will be filled in the near future, including work with the RSI 001, the MCCD 400D-250, the 425H-181, and the RSI 003 at low pressure. Some of the data given in this report, and the inferences drawn from it, are based on only one or two tubes, and should be rechecked. Other data suggest more detailed runs for better accuracy.

Two RSI thyratrons with glass interaction regions are nearing completion, and will be tested soon after construction. They will be tested by means similar to those reported above, and with optical measurements by image converter and optical spectrophotometer to watch actual quenching behavior and to inspect for possible contaminants.

With the amount of data now on hand, theoretical work with the assistance of Professors Politzer and Smullin at the Massachusetts Institute of Technology can begin, and ties between them and new experiments are expected. For use in collecting data for theoretical analysis assistance, a Langmuir probe setup may be arranged for the multifold tubes. Temperature and density measurements may be obtainable from application of both pulsed and steady probe theory to our experiment. A pulsed system will be workable only if a temporary plasma equilibrium can be reached in a time much shorter than the applied probe pulse.

A rearrangement of the magnet firing circuit is planned, with a superposition of magnetic fields from separate firing circuits. This alteration will aid in determining the relative fields and field shapes needed both for quenching a fault discharge and for providing holdoff for a time period long enough for a thyratron holdoff section to deionize and regain holdoff capability.

The Machlett ML-6544 triode will be added to the circuit to replace the 7322, since such a circuit better simulates the intended use of the RSI. The resistance now used is not an adequate model.

A quantity of additional ceramic maze material is available at EG&G and is planned for use in the near future. Sufficient variety of material is available to add a number of points to diameter and length studies.

6. REFERENCES

1. Brown, S. C. 1959. Basic Data of Plasma Physics, Massachusetts Institute of Technology. Technology Press, p. 292.

2. Thomas, J., et al. 1967. "New Switching Concepts." A final report prepared for the U. S. Army Electronics Command by EG&G. ECOM-00123-F, p. 100.

DISTRIBUTION LIST

12 Defense Documentation Center
ATTN: DDC-TCA
Cameron Station (Bldg 5)
Alexandria, VA 22314

1 Code R123, Tech Library
DCA Defense Comm Engrg Ctr
1860 Wiehle Ave
Reston, VA 22090

1 Defense Communications Agency
Technical Library Center
Code 205 (P.A. TOLOVI)
Washington, DC 20305

1 Office of Naval Research
Code 427
Arlington, VA 22217

1 Director
Naval Research Laboratory
ATTN: Code 2627
Washington, DC 20375

1 Commander
Naval Electronics Laboratory Center
ATTN: Library
San Diego, CA 92152

1 CDR, Naval Surface Weapons Center
White Oak Laboratory
ATTN: Library, Code WX-21
Silver Spring, MD 20910

1 Rome Air Development Center
ATTN: Documents Library (TILD)
Griffiss AFB, NY 13441

1 Hq, Air Force Systems Command
ATTN: DLCA
Andrews AFB
Washington, DC 20331

2 CDR, US Army Missile Command
Redstone Scientific Info Center
ATTN: Chief, Document Section
Redstone Arsenal, AL 35809

1 Commander
US Army Missile Command
ATTN: DRSMI-RE (Mr. Pittman)
Redstone Arsenal, AL 35809

3 Commandant
US Army Aviation Center
ATTN: ATZQ-D-MA
Fort Rucker, AL 36362

1 Director, Ballistic Missile Defense
Advanced Technology Center
ATTN: ATC-R, PO BOX 1500
Huntsville, AL 35807

1 Commander
HQ Fort Huachuca
ATTN: Technical Reference Div
Fort Huachuca, AZ 85613

2 Commander
US Army Electronic Proving Ground
ATTN: STEEP-MT
Fort Huachuca, AZ 85613

1 Commander
USASA Test & Evaluation Center
ATTN: IAO-CDR-T
Fort Huachuca, AZ 85613

1 Deputy for Science & Technology
Office, Assist Sec Army (R&D)
Washington, DC 20310

1 CDR, Harry Diamond Laboratories
ATTN: Library
2800 Powder Mill Road
Adelphi, MD 20783

1 Director
US Army Ballistic Research Labs
ATTN: DRXBR-LB
Aberdeen Proving Ground, MD 21005

1 Harry Diamond Laboratories, Dept of Army
ATTN: DRXDO-RCB (Dr. J. Nemarich)
2800 Powder Mill Road
Adelphi, MD 20783

1 Commander
US Army Tank-Automotive Command
ATTN: DRDTA-RH
Warren, MI 48090

1 CDR, US Army Aviation Systems Command
ATTN: DRSAV-G
PO Box 209
St. Louis, MO 63166

1 TRI-TAC Office
ATTN: CSS (Dr. Pritchard)
Fort Monmouth, NJ 07703

1 CDR, US Army Research Office
ATTN: DRXRO-IP
PO Box 12211
Research Triangle Park, NC 27709

1 CDR, US Army Research Office
ATTN: DRXRO-PH (Dr. R.J. Lontz)
PO Box 12211
Research Triangle Park, NC 27709

1 Commandant
US Army Air Defense School
ATTN: ATSA-CD-MC
Fort Bliss, TX 79916

1 Commander, DARCOM
ATTN: DRCDE
5001 Eisenhower Ave
Alexandria, VA 22333

1 Chief
Ofc of Missile Electronic Warfare
Electronic Warfare Lab, ECOM
White Sands Missile Range, NM 88002

Commander
US Army Electronics Command
Fort Monmouth, NJ 07703
1 DRSEL-GG-TD
1 DRSEL-WL-D
3 DRSEL-CT-D
1 DRSEL-TL-DT
3 DRSEL-TL-BG
1 DRSEL-TL-BG (Ofc of Record)
2 DRSEL-MS-TI
1 DRSEL-TL-D
25 Originating Office

2 MIT - Lincoln Laboratory
ATTN: Library (RM A-082)
PO Box 73
Lexington, MA 02173

1 NASA Scientific & Tech Info Facility
Baltimore/Washington Intl Airport
PO Box 8757, MD 21240

2 Advisory Group on Electron Devices
201 Varick Street, 9th Floor
New York, NY 10014

1 ITT Electron Tube Division
3100 Charlotte Avenue
Easton, PA 18042